

ANALYSIS OF A SLIT DIE RHEOMETER: PREDICTING PRODUCT FLOW AND DIMENSIONS THROUGH NUMERICAL SIMULATION

F. EDI-SOETAREDJO¹, P. J. TORLEY², R. P. G. RUTGERS¹ and B. R. BHANDARI²

¹Division of Chemical Engineering, The University of Queensland, Brisbane, QLD 4072, Australia
²School of Land and Food Sciences, The University of Queensland, Brisbane, QLD 4072, Australia

ABSTRACT

Three-dimensional modelling of flow in a two channel slit die rheometer (Vergnes et al, 1993) fitted to a twin-screw extruder has been modelled with the finite element method. The twin channel design means that the rheometer can be used to study the rheological behaviour of materials that are sensitive to thermo-mechanical changes, such as starchy products, since local shear rate within the channels can be varied without changing the flow condition in the extruder. This paper presents a method of numerical simulation that provides insight into conditions within an on-line slit die (i.e. a streamline concept for obtaining die pressure and velocity profiles, local shear rate and viscosity) and also predicts the product dimension after exit from the die. Experimental data collected with the slit die rheometer was used to determine the correlation between shear rate and apparent viscosity, calculated via a power law equation, and was used as a modelling input. On-line measurements made with the slit die rheometer provide valuable rheological data about extruded products. This data can be used for rheological modelling of flow extruder dies, allowing for more efficient die design process.

Keywords: twin-screw extruder, slit die rheometer, finite element modelling.

NOMENCLATURE

D	Diameter
h	Channel depth
K	Consistency factor
L	Total length channel/ length
L _p	Length of the piston valve
n	Power law index
P ₀	Entrance pressure
P _e	Pressure at entry of the piston valve
v	Velocity
w	Channel width
η	Viscosity
γ̇	Shear rate

INTRODUCTION

Extrusion processing has been applied in various industries (eg breakfast cereal, pet food, plastics, etc.) because it allows simultaneous mixing, shearing and heating. There are two principal components in an extrusion process: the extruder and the die. The extruder is responsible for forming the melt from the raw materials and the die determines product dimensions.

Extrusion dies are made to shape the extrudate to the desired form, for example a die with an opening in the form of an annulus is used to extrude pipe and a slit die

having a rectangular opening is used to extrude sheet. Moreover, it is possible to form more complex two or three-dimensional shapes, such as tubular, spherical or "novelty" extrudates (eg smiley face) by combining careful control of melt rheology with knowledge of the effect of die design and post die expansion. Therefore, good die design is essential to assure the product quality.

There are two important parameters in extrusion die design, namely the velocity field inside the die and the pressure drop across the die (Gupta, 2001). Knowledge of the velocity profile inside the die is essential to avoid recirculating vortices, stagnation and hence decomposition of the extruded product. Pressure field information in the die is important for a robust mechanical die design so that the internal pressure does not cause any significant change in the flow channel dimensions [Howkin et al, 1986 (a) and (b), Walter, 1992, Gupta, 2001].

Velocity and pressure fields inside the extruder die have been modelled using various approaches varying from simple models based on one-dimensional analytical solution of the differential equations, to more complex numerical techniques using the finite volume method and the finite element method (FEM). Among these approaches, FEM is currently the preferred approach for this study because it is independent of geometry and has high accuracy and flexibility, especially when dealing with non-linear problems encounter in extrusion [Walter, 1992, Hanson and Cappella, 1998].

The primary focus of this study is to present a method of numerical simulation that provides insight into conditions within an online-slit die using the streamline concept for obtaining die pressure and velocity profiles, local shear rate and viscosity and finally to predict the product dimension after exit from the die. In this study, a twin channel slit die was modelled using finite element based software package, Polyflow 3.10 (Fluent Inc., Lebanon, NH., USA). This package was chosen because it is optimised for modelling viscous flow in laminar conditions involving complex rheology and free surfaces.

SLIT DIE RHEOMETER

The basic principle of the slit die rheometer is to vary the local shear rate in the die without changing the flow conditions in the extruder. The die has two geometrically identical channels, one considered as the measurement channel and the second as a bypass channel. Each channel has a piston valve to modify the flow rate. Modifying the flow rate in the first channel by moving the piston is balanced by adjusting the piston height in the second channel in the reverse direction in order to maintain a constant entrance pressure (P₀). This slit die enables online viscosity measurement for constant thermo-mechanical treatment, which is important in the study of

the rheology of extrusion melts that are sensitive to thermo-mechanical treatment, such as starch-based product [Walter, 1992].

The twin channel slit die design was based on the on-line “Rheopac” rheometer die of Vergnes et al (1993) that was modified by Gena Nashed (personal communication). The critical die dimension are $L_p=0.01\text{m}$; $h=0.0015\text{m}$; $L=0.1\text{m}$; $w=0.0075\text{m}$, which were smaller than those used by Vergnes because of the lower throughput of the extruder used in this study (Fig. 1).

MATERIAL AND METHOD

Extrusion trials were performed with unmodified maize starch (3401 C, 74% amylopectin and 26% amylose) from Penford Australia, North Ryde, NSW.

Extrusion trials were performed in a co-rotating twin-screw extruder (Eurolab Prism KX16, Thermo PRISM, Staffordshire, U.K.), which has a barrel diameter of 0.016m (L/D ratio of 40). The following extrusion conditions were used: screw speed (200 rpm), powder feed rate (0.57 kg/h), water feed (0.24 kg/h). Water was injected into the extruder barrel in a zone right after the flour feeder, using a peristaltic pump (Masterflex L/S, Exttech Equipment Pty, Victoria, Australia). The barrel temperature profile from the feed zone to the end of the extruder barrel was 50, 90, 115, 110, 110, 110, 105, 105°C and the die was maintained at 85°C.

Extruded product density was measured using Helium Pycnometer (Micromeritics AccuPyc 1330) at room temperature. The GNOMIX PVT (Gnomix in Boulder, Colorado, USA) was used to measure the extrudate density changes in volume with changing temperature and pressure. At the average melt temperature (105°C) and the average die pressure (4.8 Mpa) the melt density in the die was calculated as 1354 kg/m³.

MODEL DESCRIPTION

A mesh describing the geometry of the slit die rheometer was built and meshed using Gambit 2.0 (Fluent Inc., Lebanon, NH, USA) (Fig. 2a). The die geometry is symmetrical about a vertical plane and a horizontal plane passing through the middle of the die. In order to save computing time, modelling was performed on a quarter of the domain of the slit die (6763 elements, which consisted of cube, tetrahedron, pyramid and prism) (Fig. 2b.).

In this simulation, the fluid was assumed to be non-Newtonian and the flow along the die was isothermal. The material properties of the starch melt were taken as a simple power-law model non-Newtonian viscous, incompressible fluid (1) [Fluent, 2001].

$$\eta = K(\dot{\gamma})^{n-1} \quad (1)$$

The viscosity of starch melt as a function of shear rate shows shear thinning behaviour. From online slit-die rheometer experiment, the value of consistency factor, K , was found to be 7379.7; and the power-law index 0.2986. Because the power-law index is lower than 0.75, Picard interpolation was used in the calculation because it gives better convergence behaviour. The experimentally determined extrudate density value of 1354 kg/m³ was used in the modelling.

To set up the finite element calculation, six boundary conditions were imposed (Fig. 2C):

- Boundary 1: Die inlet. Flow rate= 38.7 mm³/s, which is a quarter of the total flow rate.
- Boundary 2: Die wall. All components of the velocity were set to zero (no slip condition).
- Boundary 3: Horizontal symmetrical surface. Normal velocity= 0 and tangential force= 0
- Boundary 4: Vertical symmetrical surface. Normal velocity= 0 and tangential force= 0.
- Boundary 5: Free deforming surface of the extruded profile
- Boundary 6: Outlet: normal force= 0 and tangential velocity= 0.

Boundary five was a free deforming surface used to predict the product shape. This boundary had to be treated specially as internal nodes within this boundary were changing as the extrudate was produced. The Polyflow Optimesh-3D remeshing technique was chosen to remesh this boundary because this technique is able to handle the large deformations that commonly occur in extrusion processes [Fluent, 2001]. A steady state flow solution was calculated, which converged after 20 iterations with relative variable convergence was 1.10⁻⁴.

RESULT AND DISCUSSION

Figure 3 shows the simulated velocity profile on the vertical plane of symmetry in three regions, cylindrical region ($z=12\text{mm}$), conical channel ($z=35\text{mm}$) and slit channel ($z=47\text{mm}$). The melt velocity increases when the melt enters the narrower channel (as is shown by the velocity contours in Fig. 3) and reaches the highest velocity at the entrance of slit channel before the fully developed profile is observed at $z=47\text{mm}$. The melt velocity gradient near the wall increased as the channel narrows (Fig. 4). At $z=47\text{mm}$, the melt velocity was fully developed, which supports the assumption made in on-line slit die measurement that the flow is fully developed in the section under the piston valve [Vergnes, 1993] (in this case the piston position was at $z=48\text{mm}$, Fig. 1).

The melt pressure drops slightly from 3.4 MPa at $z=0\text{mm}$ to 3.3 MPa at $z=35\text{mm}$, then gradually falls until the exit of the die (Fig. 5). The slight pressure drop before the melt entered the slit channel indicated that there was some elastic deformation at the entry to the slit channels. In on-line slit die measurements the pressure drop resulting from the friction of fluid in the capillary is the only quantity that is used for viscosity calculation and therefore it is important to use Bagley correction to eliminate the entry pressure drop in the calculation [Walter, 1992].

The local shear rate observed in the modelling calculation varied from close to zero at the centre of the melt flow to a maximum shear of 12 s⁻¹ near the die wall. The local shear rate profile at the vertical plane of symmetry from the transition region to the extruded product is shown in Figure 6. Cross-sections at various points along the z-axis show that the shear rate changes proportionally to the velocity changing. Figure 8 shows that at $z=12\text{mm}$, the shear rate was close to zero along x-axis since the velocity of the melt at this point was uniform. The shear rate gradient near the wall decreases as the channel narrows (Fig. 8).

Starch melt viscosity profile exhibits a reverse trend to melt shear rate profile. The highest viscosity of 4×10^5 Pa.s was in the centre of flow and the lowest viscosity of 473 Pa.s was close to the die wall. Figure 7 shows the profile of melt viscosity. The scale is limited to the range 473 – 60000 Pa.s; melt viscosities higher than 60000 Pa.s are shown in the insert of Figure 7. The largest melt viscosity range was found in the beginning of cylindrical channel and it reduced as the melt flowed through the cylindrical channel. Figure 9 shows that the largest melt viscosity range was found in the cylindrical channel ($z = 12$ mm). The melt viscosity gradient at 4 mm to the die wall ($x = -8$ to -4 mm) in the cylindrical channel found smaller than the viscosity gradient from that point ($x = -4$ mm) to the centre of the channel ($x = 6$ mm) because starch melt experienced higher shear rate in the area close to die wall. As the melt velocity gradient increased when the melt enter the conical channel, the melt viscosity reduced ($z = 35$ mm) and was found to be nearly independent to the cross section position. When velocity of melt was fully developed in the slit channel, melt viscosity remained within 2000 to 10000 Pa.s.

From the modelling result on the extrudate shape prediction, it was found that there was swelling in the y-direction but shrinking in the x-direction (Fig.10). The colours and contours in the picture show the normal velocity profile of the extrudate product. It is shown in Figure 10B (in mesh display) that there was deformation of the product when the product exited the die before the product maintained its shape. The modelling result was in good agreement with the extrusion experiment, which is shown in Figure 10C and 10D.

CONCLUSION

FEM numerical simulation had been performed for a twin channel slit die in Polyflow 3.10 to analyse the melt flow

and to predict extrudate shape. The simulated velocity field supports the assumption made in slit-die measurement. The pressure field result shows the importance of using the Bagley correction.

REFERENCES

- Gupta, M., (2001) Effect of elongational viscosity on die design for plastic extrusion. *Journal of Reinforced Plastics and Composites*, 20(17): 1464-1472.
- Hanson, D and R Cappella., (1998), Extrusion flow analysis software verification. *Proceedings of ANTEC*, 3471-3474.
- Howkins, M D, R G Morgan, and J F Steffe., (1986) Extrusion die swell of starch doughs. *American Society of Agricultural Engineer.*
- Howkins, M D and R G Morgan., (1986), Similitude approach to food extrusion die flow problems. *American Society of Agricultural Engineers.*
- Polyflow Reference Manual, Fluent, 2001.
- Vergnes, B, G Della Valle, and J Tayeb., (1993), A specific slit die rheometer for extruded starchy products. Design, validation and application to maize starch. *Rheologica Acta*, 32: 465-476.
- Walter, M., (1992), Extrusion die for plastics and Rubber. 2nd ed., New York, Hanser.

ACKNOWLEDGEMENTS

FES wishes to thank AusAID for the financial support through an Australian Development Scholarship. The authors would like to thank Nicolas Clemeur for valuable discussion about Polyflow simulation, Dr Timothy Nicholson for his contribution in this paper and Gena Nashed with online slit-die rheometer experiment set-up. Dr Rutgers thanks Polyflow S.A. for the use of a free Polyflow licence.

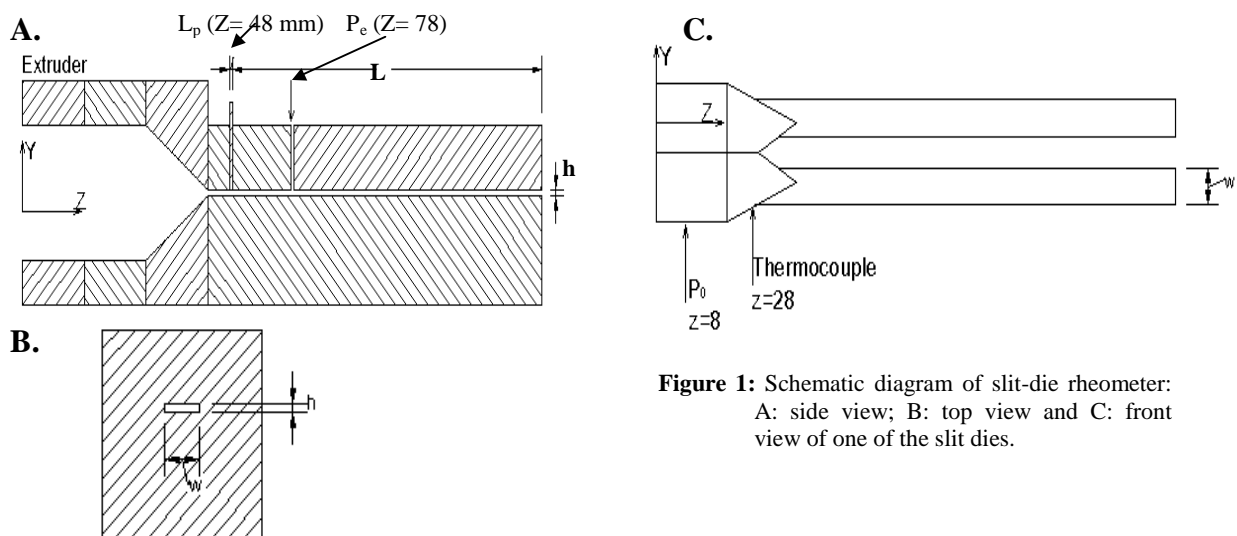


Figure 1: Schematic diagram of slit-die rheometer: A: side view; B: top view and C: front view of one of the slit dies.

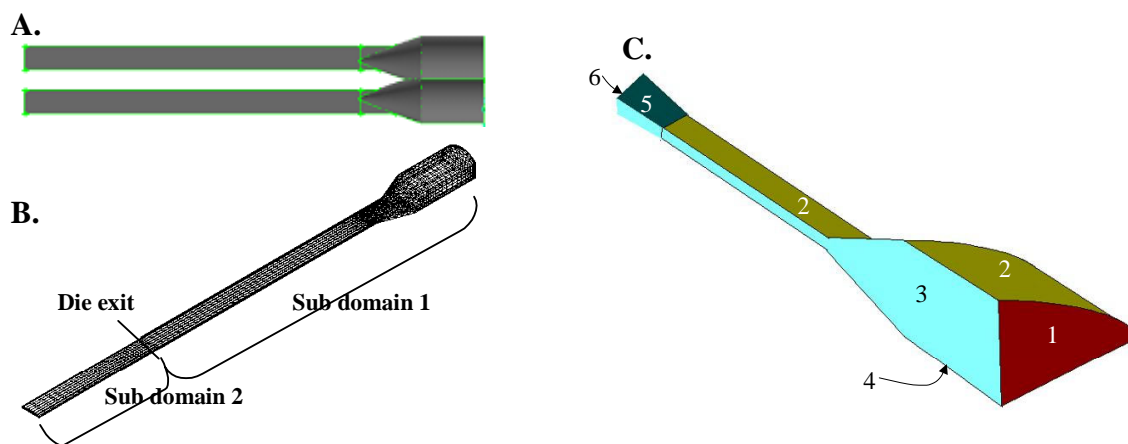


Figure 2: A: Slit-die rheometer geometry; B: mesh of a quarter of slit-die rheometer; C: boundary conditions position.

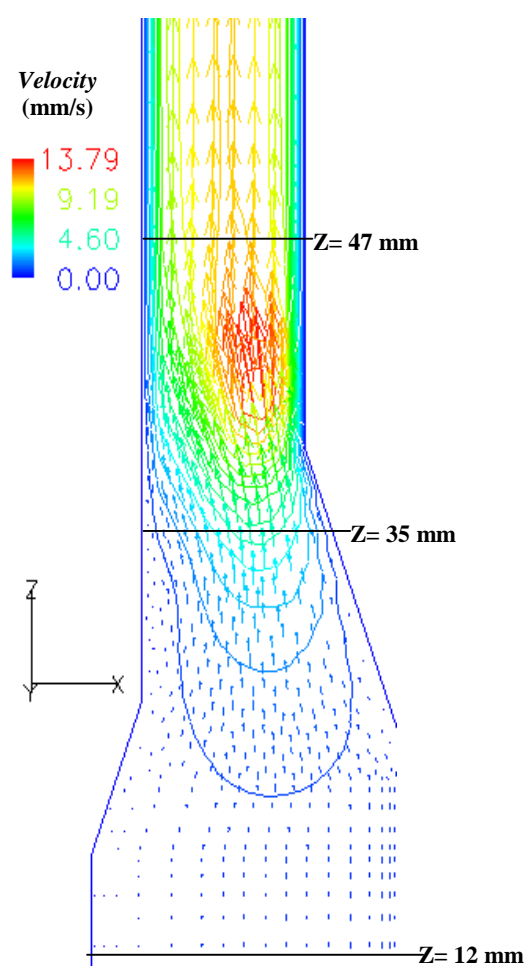


Figure 3: Velocity profile at the vertical plane of symmetry in the transition region from conical channel to slit channel

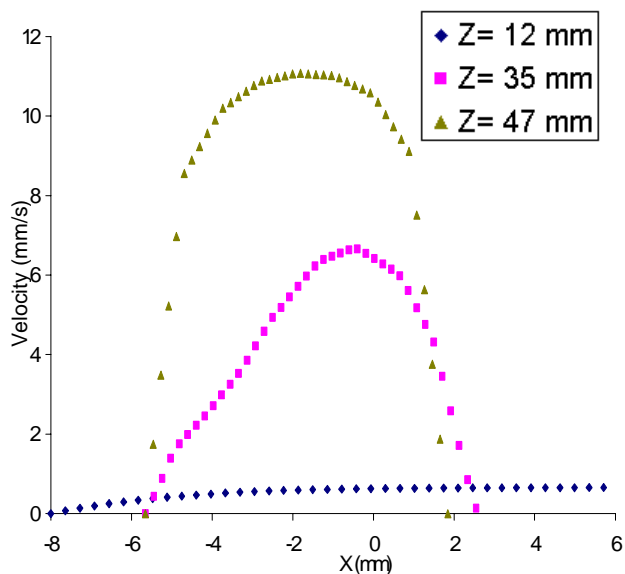


Figure 4: Normal velocity curve x-axis at various points along the z-axis.

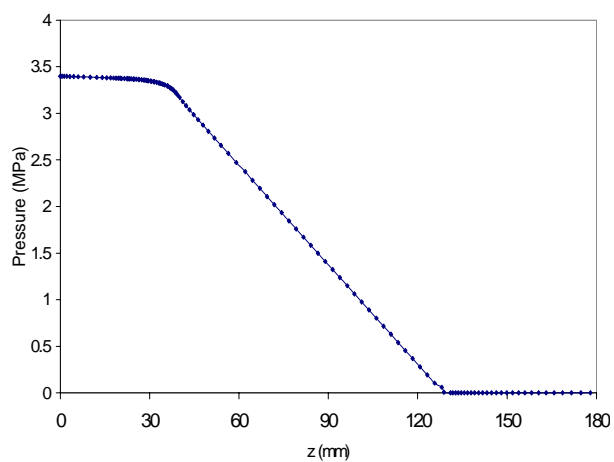


Figure 5: Pressure profile along z-axis.

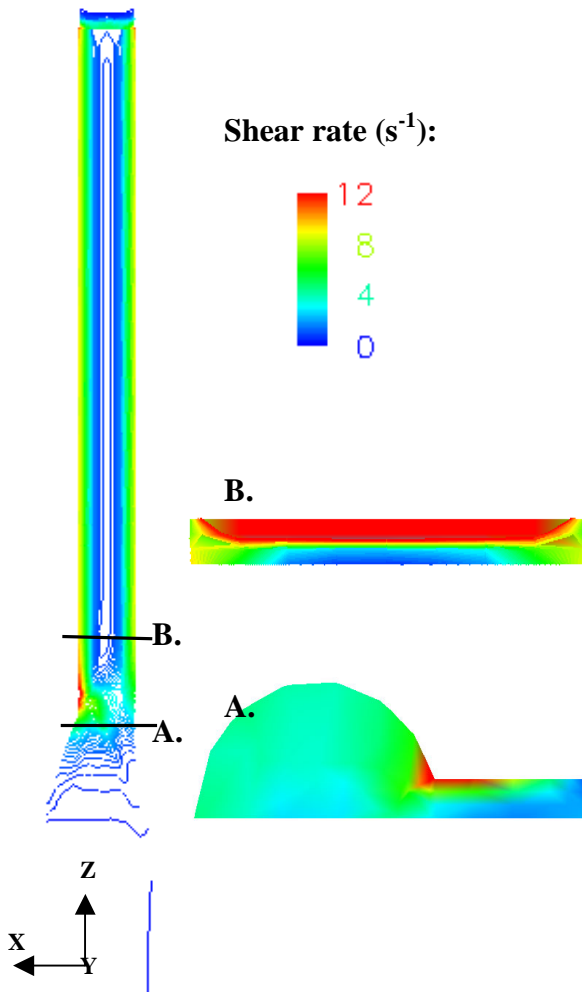


Figure 6: Local shear rate contour profile at vertical plane of symmetry from conical channel to slit channel. A, B and C are x-slices of local shear rate profile at some points of z-axis, 35.7, 39.6 and 47 mm, respectively.

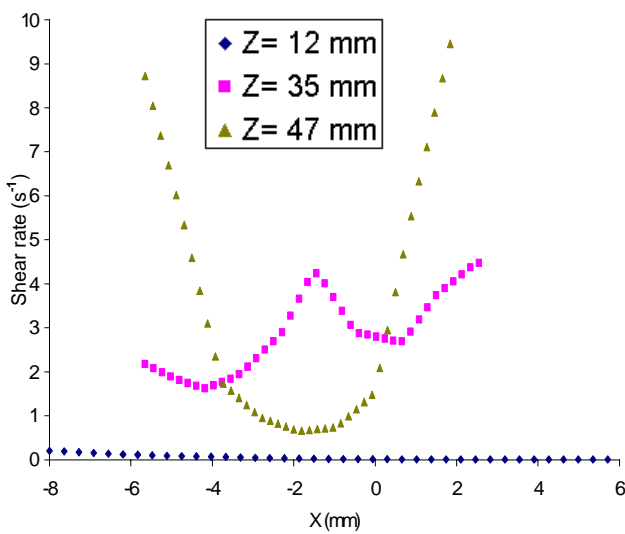


Figure 8: Local shear rate curve along x-axis of slit die at various points of z-axis.

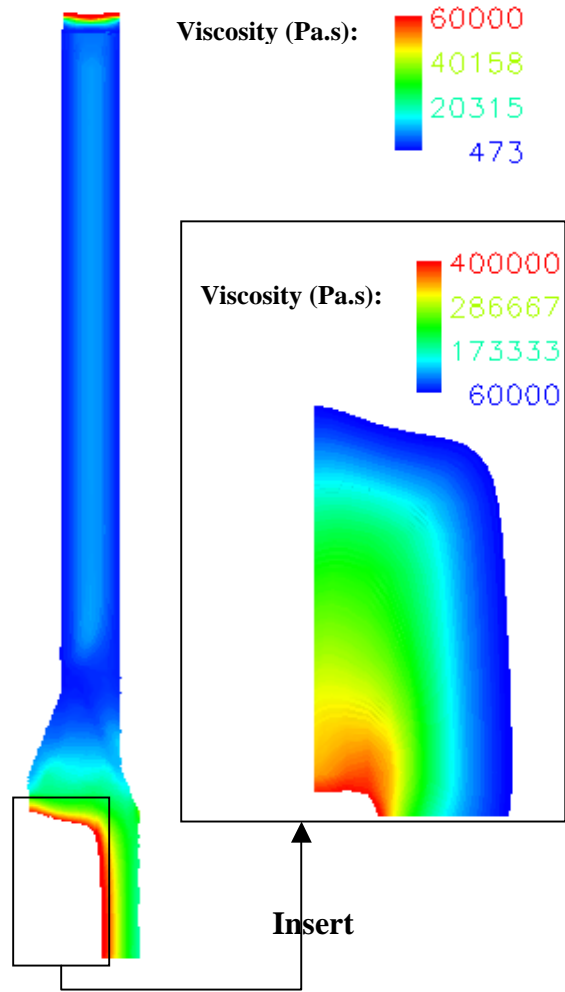


Figure 7: Viscosity contour profile at the vertical plane of symmetry of the slit die, showing a viscosity range 473 – 60000 Pa.s.

Insert: Viscosity profile showing a viscosity range 60000 – 400000 Pa.s (which occurs in the cylindrical channel).

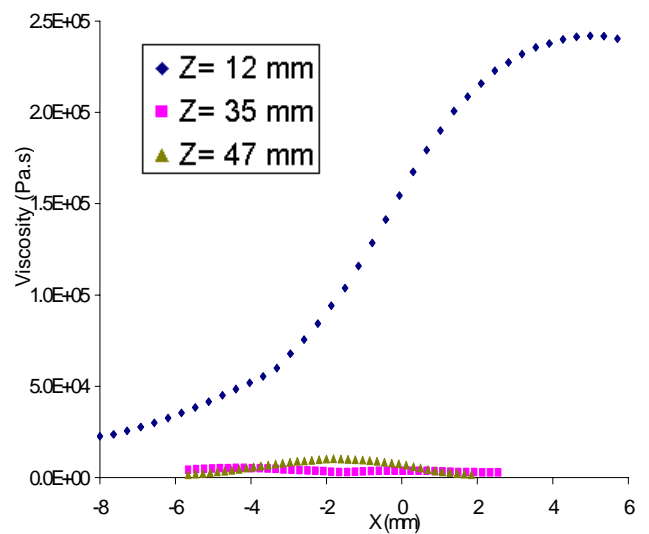


Figure 9: Viscosity curve along x-axis of slit die at various points of z-axis.

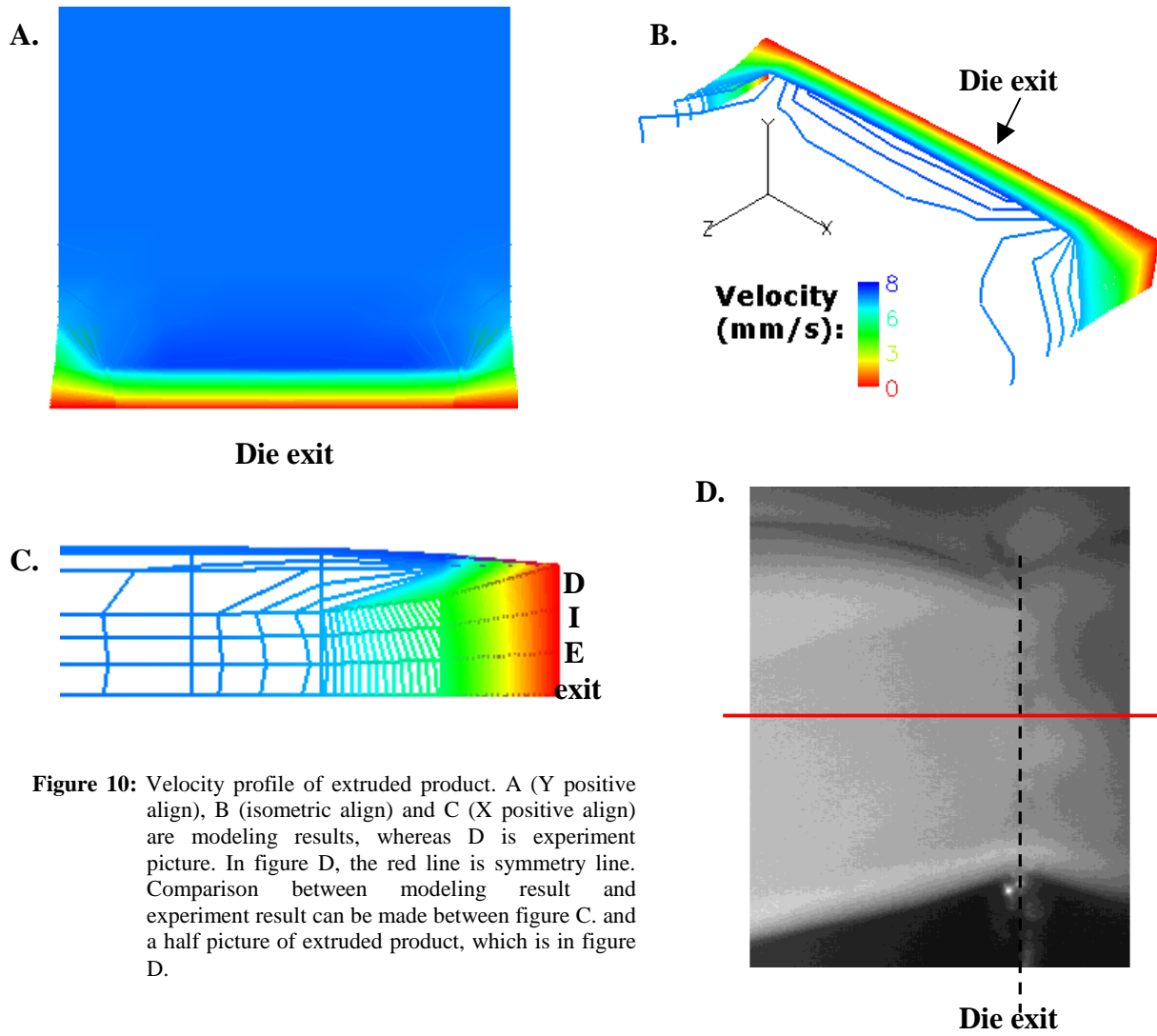


Figure 10: Velocity profile of extruded product. A (Y positive align), B (isometric align) and C (X positive align) are modeling results, whereas D is experiment picture. In figure D, the red line is symmetry line. Comparison between modeling result and experiment result can be made between figure C. and a half picture of extruded product, which is in figure D.